Social reactivation of fear engrams enhances memory recall

Abby Basya Finkelstein[a,b,1], Héloïse Leblanc[a,c,2], Rebecca H. Cole[a,2], Troy Gallerani[a,c], Anahita Vieira[a,d], Yosif Zaki[a,e], and Steve Ramirez[a,1]

For group-living animals, the social environment provides salient experience that can weaken or strengthen aspects of cognition such as memory recall. Although the cellular substrates of individually acquired fear memories in the dentate gyrus (DG) and basolateral amygdala (BLA) have been well-studied and recent work has revealed circuit mechanisms underlying the encoding of social experience, the processes by which social experience interacts with an individual's memories to alter recall remain unknown. Here we show that stressful social experiences enhance the recall of previously acquired fear memories in male but not female mice, and that social buffering of conspecifics' distress blocks this enhancement. Activity-dependent tagging of cells in the DG during fear learning revealed that these ensembles were endogenously reactivated during the social experiences in males, even after extinction. These reactivated cells were shown to be functional components of engrams, as optogenetic stimulation of the cells active during the social experience in previously fear-conditioned and not naïve animals was sufficient to drive fear-related behaviors. Taken together, our findings suggest that social experiences can reactivate preexisting engrams to thereby strengthen discrete memories.

engram | optogenetics | hippocampus | memory | amygdala

For social species such as humans and rodents, conspecific interactions pervasively shape emotion (1–3), attention (4), and cognitive ability (5–8). Higher-order cognitive processes such as memory within a social brain are thus interlaced with social influences. Traditional laboratory rodent cages offer a limited but nonetheless rich multimodal landscape of communication, including auditory calls (9–12), chemical signaling (13, 14), and tactile stimulation (15, 16). The absence of such social encounters in singly housed animals results in cognitive impairments and depression-like phenotypes (17), likely obscuring how the social brain has evolved to function. It is thus important to understand the relationship between social context and how individuals process memories. As social interaction recruits hippocampal (18) and amygdalar (19) circuitry that also serves as hubs for nonsocial memory traces (20–24), we hypothesized that preexisting ensembles in these regions can be modulated by social experiences and lead to changes in memory expression.

Results and Discussion

Postlearning Social Stress Amplifies Behavioral Expression of Fear Recall in a Sex-Dependent Manner. To assess how social experiences influence existing memories, male and female mice were subjected to social or nonsocial salient events in the day between contextual fear conditioning (FC) and memory recall tests (Fig. 1*A*). A socially salient experience was provided in various forms: interaction with an unfamiliar juvenile intruder placed in the subject's home cage (25, 26) to create a salient and mildly stressful event (juvenile intruder group); interaction with a recently shocked cagemate in the home cage to simulate a stressed familiar conspecific (full interaction group); indirect nonvisual and nonphysical exposure to a recently shocked cagemate in the home cage behind a one-way mirror that permits unidirectional visual access for the shocked mouse to see the cagemates on the other side, to simulate ambient exposure to conspecifics' stress (one-way mirror group; *SI Appendix*, Fig. S1); and exposure to a recently shocked cagemate in the home cage through the same mirror covered in opaque black material to block both sides' visual access (opaque group). A nonsocial, salient experience was provided in the form of individual restraint stress in a tube (restraint group), while a social but nonstressful experience was provided via interaction with a cagemate in the home cage (cagemate control) or with a female mouse (female exposure) (*Materials and Methods*). Additional control groups included mice that did not experience any events in the day between FC and recall (neutral group), and mice that were exposed solely to the novel objects presented in the experimental groups without the associated salient events: the one-way mirror object (mirror no mouse

Significance

Social interactions can bolster and protect memory performance. However, the relationship between social stimuli and individually learned memories remains enigmatic. Our work reveals that exposure to a stressed, naïve nonfamiliar conspecific or to the ambient olfactory–auditory cues of a recently stressed familiar conspecific induces reactivation of the cellular ensembles associated with a fear memory in the hippocampus. Artificially stimulating the hippocampal ensemble active during the social experience induces fearful behaviors in animals that have previously acquired a negative memory, revealing the interaction between individual history and social experience. The neural resurgence of fear-driving ensembles during social experiences leads to a context-specific enhancement of fear recall. Our findings provide evidence that unlike direct stressors, social stimuli reactivate and amplify an individual's memories.

[1]To whom correspondence may be addressed. Email: afinkelstein@fas.harvard.edu or dvsteve@bu.edu.
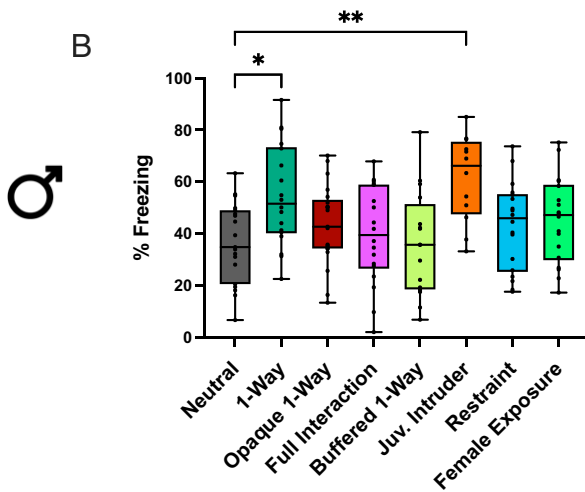
[2]H.L. and R.H.C. contributed equally to this work.
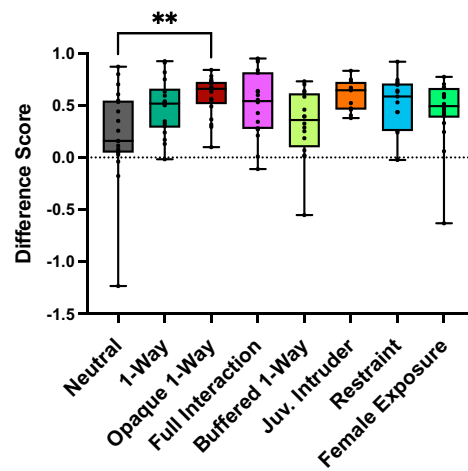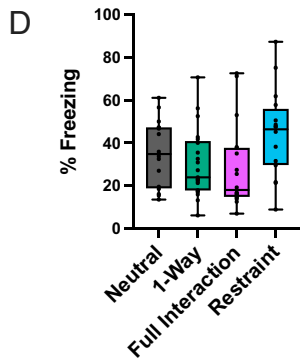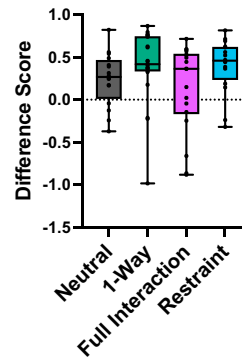
Fig. 1. Social stimuli modulate subsequent fear recall in a sex-dependent manner. (*A*) Schematic representation of the behavioral schedule. (*B* and *D*) Freezing levels during a 5-min fear recall test for males (*B*) and females (*D*). Males: one-way ANOVA$F_{(7, 132)}$ = 3.841, P = 0.0008; Holm–Sidak's multiple comparisons: ***P = 0.0011 for neutral vs. juvenile intruder; **P = 0.0114 for neutral vs. one-way mirror. Females: one-way ANOVA$F_{(3, 67)}$ = 2.626, P = 0.0575. (*C* and *E*) Difference scores, defined as [(freezing in recall test) − (freezing in generalization test)]/(freezing in recall test) for males (*C*) and females (*E*). Males: Kruskal–Wallis statistic = 17.40, *P = 0.0150; Dunn's multiple comparisons: **P = 0.0041 for neutral vs. opaque. Females: ANOVA$F_{(3, 67)}$ = 1.691, P = 0.1773. Boxes extend from the 25th to 75th percentiles, lines show medians, and whiskers extend from minimum to maximum. See also *SI Appendix*, Figs. S2 and S3.

group) and the restraint tubes (tubes group) to determine the impact of the novelty component (*Materials and Methods*).

Males exhibited higher levels of baseline freezing and froze more than females after the first two shocks of FC, after which freezing levels were similar (*SI Appendix*, Fig. S2*B*), corroborating tone-cued experiments that report higher levels of freezing in males during acquisition (27). For males, all control groups exhibited similar freezing during recall and generalization tests to the neutral group (*SI Appendix*, Fig. S2 *C* and *D*), indicating that the novel objects, as well as the nonstressful social experiences, did not impact recall. The restraint group also performed similar during recall and generalization tests to the neutral group, suggesting that direct physical stress does not alter a previously established fear memory. We chose a short bout of immobilization (2 min) to match the intensity of stress with the much milder socially stressful experiences. However, a longer bout of immobilization (30 min) has previously been shown not to impact fear recall if applied 90 min post FC (28). Both the juvenile intruder and one-way mirror groups froze more than the neutral group during the recall test (Fig. 1*B*), despite similar levels of generalization (Fig. 1*C*), indicating that specifically social events enhance recall. These results extend the recent finding that observing a conspecific rat or human undergo an unconditioned stimulus (US) of electric shock reinstates context-specific fear memory (28), suggesting that a conspecific's non–US-specific stressed state can also strengthen observers' fear memory.

We found that there was a subsequent enhancement of recall only if the stressed cagemate could see the experimental mice through a one-way mirror; the opaque group (in which a wall obscured the stressed cagemate's visual access) froze the same as the neutral group during recall but exhibited higher difference scores, suggesting reduced generalization (Fig. 1*C*). The blocking of enhanced recall when the stressed cagemate cannot see the other mice suggests the intriguing possibility that distressed mice emit different auditory–olfactory stimuli based on their perceived social context, that is, producing more distressed signals when familiar conspecifics are nearby and available to buffer this distress (29).

The full interaction group also froze the same as the neutral group during recall, indicating that physical interaction between the experimental mice and stressed cagemate blocked the effect on recall. It is crucial to note that physical interaction with a stressed familiar cagemate is not simply a heightened version of either the passive exposure to stressful emissions or of the interaction with an unfamiliar juvenile intruder mouse. In light of recent work on social buffering (30, 31), especially via physical interactions such as allogrooming (29), we hypothesized that full interaction permitted the experimental mice to buffer the shocked cagemate's distress, and the subsequently reduced stress response failed to evoke the strengthening of cagemates' fear recall. To test this hypothesis directly, we repeated the one-way mirror protocol but placed one of the cagemates on the same side as the shocked mouse, thus allowing social buffering of the shocked mouse but maintaining the same conditions for the experimental mice on the other side (buffered one-way group). As predicted, the buffered one-way group froze the same as the neutral group, indicating that the social buffering permitted in the full interaction group is sufficient to explain the blocking of effect on the experimental mice's recall.

Females, on the other hand, exhibited no effect of either social or nonsocial experience on freezing during recall (Fig. 1*D*). The only difference in memory occurred for generalization

of fear; both the mirror no mouse and tube control groups exhibited elevated difference scores compared with the neutral group (*SI Appendix*, Fig. S2*F*), indicating that when presented in the absence of other salient experience, novel object exposure following FC can reduce the generalization of fear in females. The lack of effect of social stressors on females could be due to either a difference in cues emitted by the shocked females compared with the shocked males, to a difference in the response of cagemates to these cues, or a combination of both. Further experiments analyzing the ultrasonic vocalizations and chemical cues would enable clarification of this sex difference and testing of our hypothesis that male stressed mice emit different cues when unable to perceive social context behind the opaque wall.

These results demonstrate that intervening experiences between FC and recall can impact the intensity and context specificity of fear expression in a sex-dependent manner. Social exposure to conspecifics' distress, but not direct physical stressors, can enhance fear recall in males but not females. It is important to note that in group-housed animals, a memory acquired via FC could incorporate social stimuli produced in the home cage following conditioning. These social cues associated with the fear memory can feasibly act as a reminder cue, facilitating the enhancement of individually acquired fear memory via conspecifics' stress. Future work could reveal a putative window in which social cues are integrated with a fear memory by singly housing mice for varying lengths of time after FC. The length of time should be carefully titrated to prevent possible confounds: exposure to intruders or shocked mice could be a qualitatively different experience for socially isolated mice, and social isolation induces a depressive phenotype that alters affective processing. If social experiences proximate to fear learning lead to the enhancing effect of social stress on fear memory, fear memories formed in group-living animals in the wild would incorporate surrounding social cues and thus be vulnerable to future enhancement via social stressors.

Socially Salient Events Reactivate Ensembles Previously Active during FC. To test the hypothesis that fear memories are reactivated in the dentate gyrus (DG) during the social experience for males and not for females, we used a cFos-based activity-dependent viral strategy (Fig. 2*A*) to track fear ensembles processed in the DG (dorsal DG; dDG; *Materials and Methods*) and basolateral amygdala (BLA) (the basolateral nucleus proper; *Materials and Methods*) post FC (see representative images in Fig. 3*B* and *SI Appendix*, Fig. S4). As predicted, females did not exhibit reactivation of the DG fear trace during the social experience (Fig. 2*F*), while males exhibited significant reactivation during both types of social experience (one-way mirror, 4.8× greater than chance; juvenile intruder, 4.3× greater than chance) (Fig. 2*D*). For males, juvenile intruder groups had more active cells, as identified by cFos expression, than one-way mirror groups in the DG (Fig. 2*C*). The increased level of DG activity during exposure to a juvenile intruder compared with a stressed cagemate behind a one-way mirror (Fig. 3*D*), despite both experiences occurring in the animal's home cage, highlights the DG's role in encoding experiences beyond physical contexts per se (32). We posit that the higher level of activity in the DG during exposure to a juvenile intruder reflects the richness of direct social interaction during the juvenile intruder's presence that is not permitted in the one-way mirror paradigm.

Neither sex demonstrated DG fear trace reactivation during the nonsocial stressors of restraint or immediate shock (Fig. 2 *D* [DG] and *F*), and previous work shows that fear trace
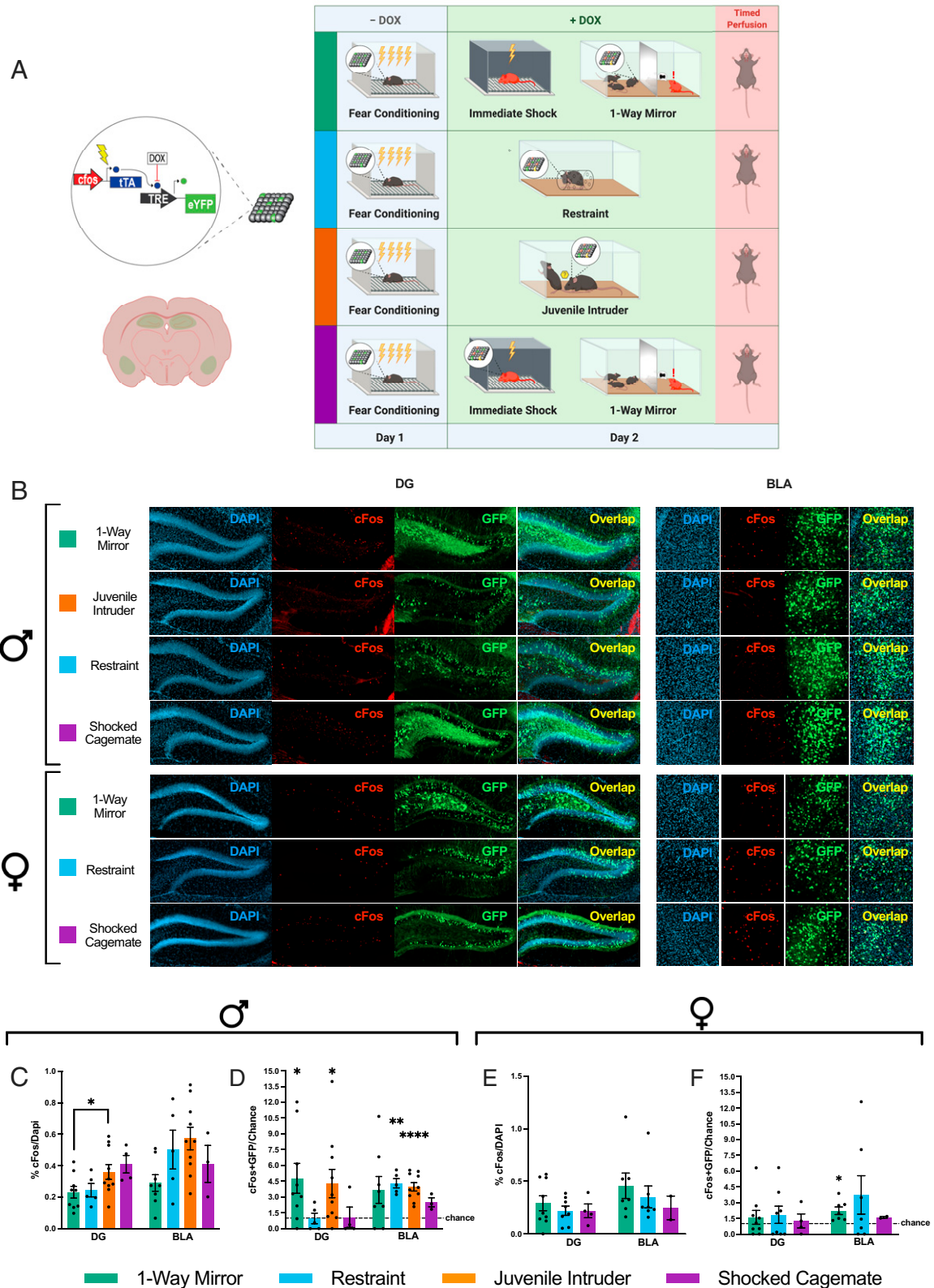
Fig. 2. Socially salient but not directly stressful experiences reactivate preexisting fear ensembles. (A) Schematic representation of the doxycycline (DOX)-mediated viral tagging construct (Left) and experimental design (Right). (B) Representative confocal images of DG and BLA histology visualizing cFos-tTa + Tre-EYFP–positive cells (active during FC; green) and cFos-positive cells (active during the different types of stress exposure; red). (C and E) Percentage of cFos-positive cells over DAPI-positive cells across brain regions in males and females. Males: DG: one-way ANOVA$F_{(3, 24)}$ = 3.028, P = 0.0490, Holm–Sidak's multiple comparisons: *P = 0.0339 for juvenile intruder vs. one-way mirror; BLA: one-way ANOVA$F_{(3, 22)}$ = 2.710, P = 0.0697. Females: DG: one-way ANOVA$F_{(2, 18)}$ = 0.4501, P = 0.6445; BLA: ANOVA$F_{(2,13)}$ = 0.4962, P = 0.6199. (D and F) Degree of overlap between the two labeled populations normalized over chance (% cFos/DAPI × % EYFP/DAPI). One-sample t tests. Males: DG: juvenile intruder: t = 2.436, degrees of freedom (df) = 9, *P = 0.0376; one-way mirror: t = 2.656, df = 8, *P = 0.0290. BLA: juvenile intruder: t = 7.411, df = 9, ****P < 0.0001; restraint: t = 7.462, df = 4, **P = 0.0017. Females: BLA: one-way mirror: t = 3.387, df = 6, *P = 0.0147. See details for nonsignificant results in *SI Appendix, Supplementary Text*. Data are shown as mean ± SEM. Dotted lines represent chance. See also *SI Appendix, Fig. S4*.
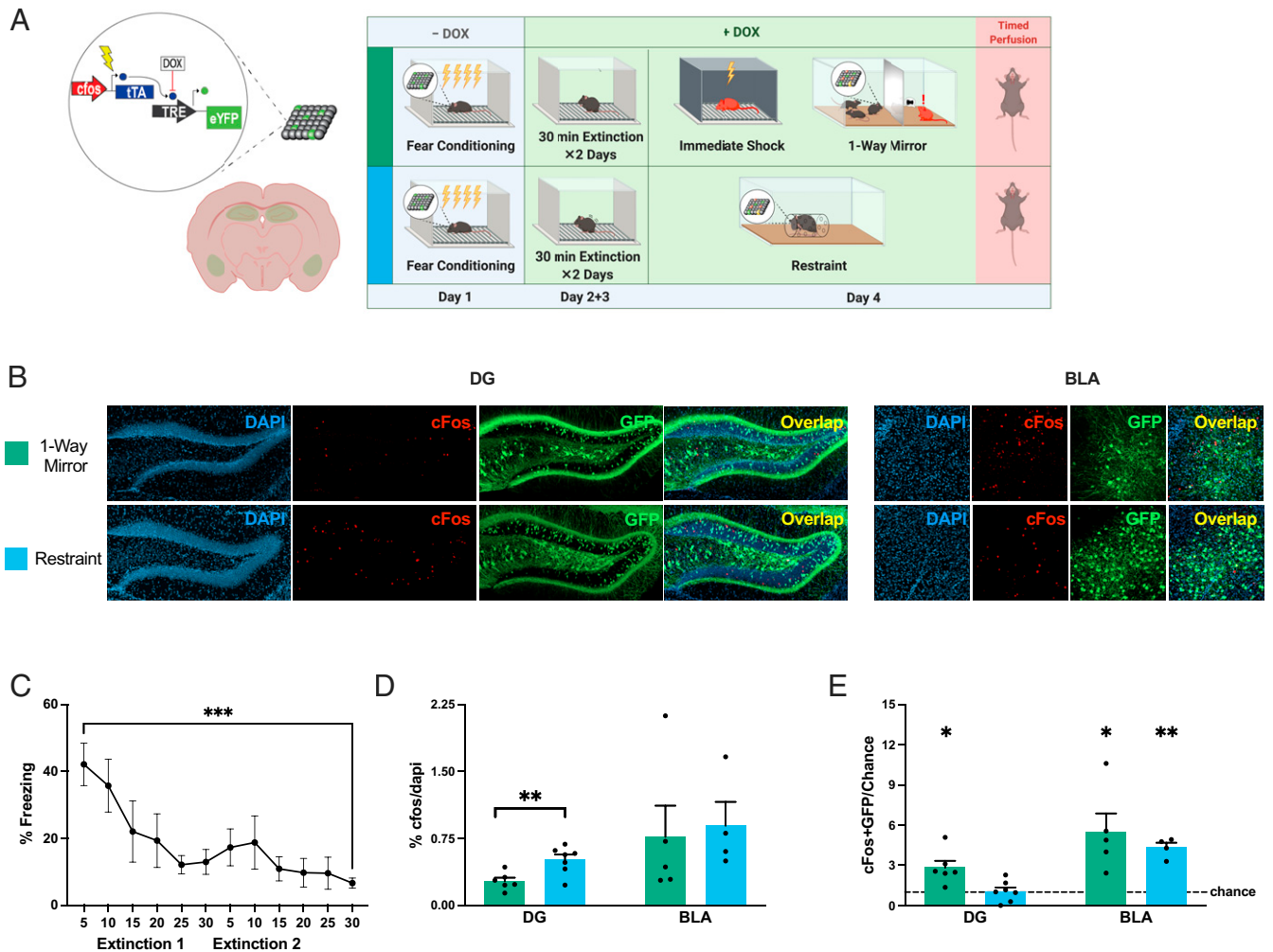
Fig. 3. Socially salient experiences reactivate fear ensembles post fear extinction. (*A*) Schematic representation of the DOX-mediated viral tagging construct (*Left*) and experimental design (*Right*). (*B*) Confocal visualization of DG and BLA histology showing cFos-tTa + Tre-EYFP–labeled cells (active during FC; green) and cFos$^+$ cells (active during the different types of stress exposure; red). (*C*) Freezing throughout extinction training (repeated-measures one-way ANOVA $F_{(3.230, 25.84)}$ = 5.165, P = 0.0054, Holm–Sidak's multiple comparisons for first vs. last 5 min, n = 9, t = 5.688, ***P = 0.0005). (*D*) Percentage of cFos$^+$ cells per DAPI$^+$ cells (DG: t test, t = 3.268, df = 11, **P = 0.0075; BLA: t test, t = 0.2716, df = 7, P = 0.7938). (*E*) Degree of overlap between the two labeled populations normalized over chance (% cFos/DAPI × % EYFP/DAPI). One-sample t tests. DG: restraint: t = 0.195, df = 6, P = 0.8516; one-way mirror: t = 3.67, df = 5, *P = 0.0153. BLA: restraint: t = 9.031, df = 3, **P = 0.0029; one-way mirror: t = 3.257, df = 4, *P = 0.0312. The dashed line represents chance. Data are shown as mean ± SEM.

reactivation does not occur in neutral contexts (33), supporting the socially specific nature of this reactivation. Conversely, in the BLA, both the juvenile intruder and restraint groups displayed reactivation of tagged cells in males (Fig. 2 *D*, BLA), suggesting that the common denominator of direct physical stress in the form of restraint or interaction with an intruder might recruit amygdalar ensembles also activated during FC the previous day. However, females in the one-way mirror group also displayed a modest but significant reactivation of tagged cells in the BLA (i.e., ~2× greater than chance, whereas the above-mentioned males displayed a ~4× greater than chance overlap) (Fig. 2F). Although our immediate-early gene–mediated resolution of the reactivated population does not permit within-region subdivision of functionally distinct subsets of a fear engram, the result that the BLA ensemble is more active than the DG ensemble during other experiences suggests that these reactivated components of the BLA fear ensemble are involved in processes other than driving acute fear responses. This idea is further supported by the discorrelation of overlaps in the BLA from overlaps in the DG in both sexes (*SI Appendix, Supplementary Text*) and corroborated

by the optogenetic stimulation experiment described below (Fig. 4).

To test whether the reactivation of the fear trace in males occurred only during events happening directly after FC, we also tracked reactivation of the fear memory following a 2 d extinction protocol (Fig. 3*A*; see representative images in Fig. 3*B*), after which mice froze significantly less in the fear context (Fig. 3*C*). The percentage of cFos$^+$ cells in the DG was slightly but consistently higher during nonsocial restraint stress than during the social experience (Fig. 3 *D*, *Left*), indicating a higher level of overall DG activity. Similar to preextinction, the DG fear ensemble was reactivated during the social experience but not during nonsocial restraint, and the BLA fear ensemble was reactivated during nonsocial restraint (Fig. 3*E*). Unlike our preextinction results, postextinction the BLA fear ensemble was also reactivated during the one-way mirror experience (Fig. 3*E*). It is important to note that our data indicate that a significant portion of the fear ensemble was reactivated and may not reflect whether the reactivated subset of cells was the same or different across these experiences.

Collectively, these data suggest that specifically social situations reactivate subsets of fear ensembles in the DG for males and not

females, and do so even after extinction training. Strikingly, the degree of DG cellular reactivation during the social encounter in males both before and after extinction was similar to previously reported results in animals reexposed to the original fear context (34). These results are consistent with the theory that endogenous reactivation of fear ensembles enhances recall (35) and is the mechanism by which multiple exposures to the contexts (36) or cues (37) present during conditioning can strengthen memories in the days after learning. We show that this reactivation does not occur during nonsocial physical stress, and previous work has shown that it does not occur in neutral contexts (33), supporting the idea of a causal relationship between reactivation and enhanced recall. Given the malleability of engrams (38, 39), the natural reactivation of a fear memory ensemble during a stressful social experience could plausibly add additional negative valence from the current experience to the representation of the former, explaining why a single negative social encounter enhances fear whereas multiple exposures to associated neutral contexts (36) are necessary for enhancement.

Stressful Social Situations Activate Fear-Driving DG Ensembles in Previously Fear-Conditioned Mice. Next, we aimed to investigate the functional properties of the cells which were active during exposure to a stressed cagemate in previously fear-conditioned animals. Fear ensemble reactivation in the DG was correlated specifically with the social experiences that heightened recall, while reactivation in the BLA was more variable. Thus, we hypothesized that the fear ensembles reactivated in the DG were composed of fear-activating cells while the ensembles reactivated in the BLA were composed of non–fear-driving components of the ensemble. We predicted that the fear ensembles reactivated during social stress in the DG, but not in the BLA, would cause the cells tagged during this period to drive fear behaviors when optogenetically stimulated. To this end, we tagged DG or BLA cells with channelrhodopsin-2 (ChR2) during our one-way mirror paradigm or during a neutral home cage period (*Materials and Methods* and Fig. 4 *A–D*). To ensure that we were not capturing a persistent fearful state but rather the reemergence of a fear ensemble, we chose to first
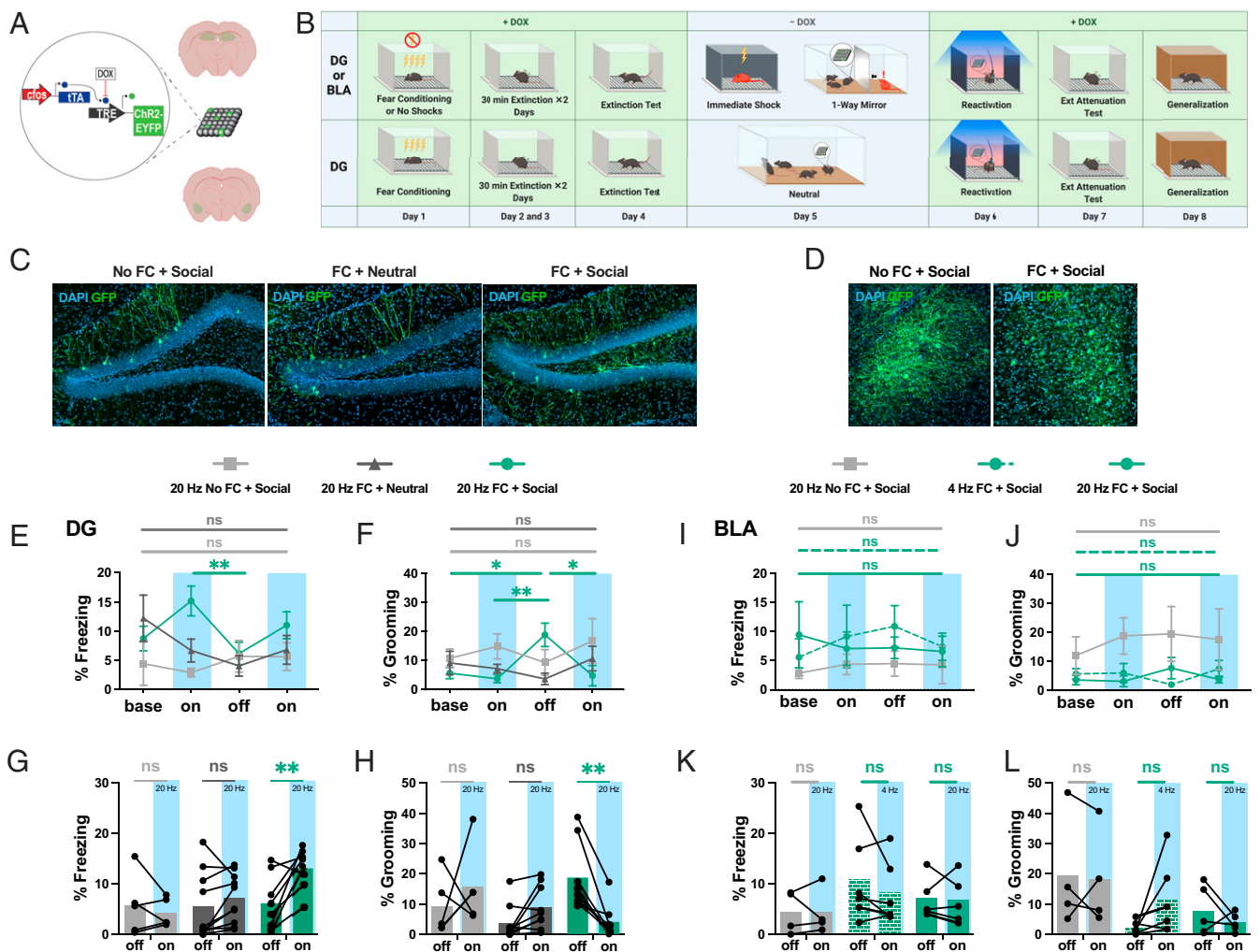

Fig. 4. DG ensembles active during social stress drive fear only in previously fear-conditioned mice. (*A*) Schematic representation of activity-dependent engram tagging strategy. (*B*) Behavioral schedule. (*C* and *D*) Representative images of DAPI⁺ cells (blue) and Chr2-EYFP⁺ cells (green) in the DG (*C*) and BLA (*D*). (*E* and *I*) Percent freezing levels throughout optogenetic stimulation of cells active in the DG (*E*) and BLA (*I*): two-way ANOVA, Holm–Sidak's multiple comparisons: for fear-conditioned DG first light-on vs. light-off: $t = 3.821$, *$P = 0.0385$. (*F* and *J*) Percent self-grooming levels throughout optogenetic stimulation in the DG (*F*) and BLA (*J*): two-way ANOVA, Holm–Sidak's multiple comparisons: for fear-conditioned DG for light-off vs. baseline: $t = 2.897$, *$P = 0.0211$; vs. first light-on: $t = 3.330$, **$P = 0.0091$; vs. second light-on: $t = 2.09$, *$P = 0.0153$. (*G* and *K*) Percent freezing levels for the light-off and the averaged light-on sessions in the DG (*G*) and BLA (*K*): two-way ANOVA, Holm–Sidak's multiple comparisons: for fear-conditioned DG light-on vs. light-off: $t = 4.072$, **$P = 0.0018$. (*H* and *L*) Percent self-grooming levels for the light-off and the averaged light-on sessions in the DG (*H*) and BLA (*L*): two-way ANOVA, Holm–Sidak's multiple comparisons: for fear-conditioned DG for light-on vs. light-off: $t = 3.5578$, **$P = 0.006$. Data are shown as mean ± SEM in *E*, *F*, *I*, and *J*. ns, not significant. Detailed statistics are shown in *SI Appendix, Supplementary Text*. See also *SI Appendix*, Fig. S5.

employ a 2 d extinction protocol before tagging the cells active during the social or neutral experience. As we show in Fig. 3, this timing still results in reactivation of the FC ensemble. The following day, the tagged ensembles were stimulated in a novel context to test their capacity to drive fearful behavior.

In support of our hypothesis, 20-Hz stimulation of the DG ensembles active during the social experience in previously fear-conditioned animals drove higher levels of freezing during the light-on sessions (Fig. 4*J*) as well as increased self-grooming (Fig. 4*K*) in the light-off period following stimulation, which is thought to reflect a dearousing behavioral state (40). To ensure that this effect was not due simply to negatively valenced cells active during social stress or active post FC regardless of social experience, we showed that fear behaviors were not induced by either stimulation of cells active in a social setting without prior FC or of cells active in a neutral setting after FC (Fig. 4*K*). The size of the labeled ensembles did not differ between any of these three groups (*SI Appendix*, Fig. S5*E*), indicating that DG activity levels were generally similar and it was not the number of tagged cells but their functionality as fear-driving cells that induced fear. In the context of the social experience, the functional capacity of the active ensembles in the DG to drive obvious fear behaviors was quiescent (see the example in Movies S1 and S2); however, we postulate that the more nuanced documented deficits in social interaction following trauma (41–44) could in part be driven by DG fear ensemble activation.

The coactivation of ensembles leads to coallocation and the linking of memories, as shown in both mouse (45) and human (46) studies. Our data suggest that during salient social experiences, the DG is concurrently reactivating a preexisting fear engram and processing the current social stimuli (Fig. 2). We therefore posit that the reactivated subset of the fear ensemble was coallocated to form part of the ensemble encoding the social encounter, perhaps explaining why the total number of cells active during the social exposure was similar regardless of prior FC (Fig. 4*I*) and why stimulation drove fearful behaviors only in the previously fear-conditioned animals (Fig. 4 *J* and *K*).

On the other hand, the number of tagged cells in the BLA was higher during social stress if mice had been previously fear-conditioned (*SI Appendix*, Fig. S3*F*), suggesting that the combination of prior FC and social stress leads to heightened amygdalar activity. This is consistent with the notion that sustained amygdalar hyperactivity underlies persistent potentiation of fear and anxiety after stressful events (47); in rats, prior stress reduces inhibitory control in the BLA, increasing excitability and plasticity (48). Although stimulation of the BLA fear engram drives freezing (20), counterbalanced 20- and 4-Hz stimulation of cells tagged during social stress did not cause freezing or grooming (Fig. 4*H*), indicating that the amygdalar cells that were active during both FC and social stress (Fig. 3*E*) did not comprise the portion of the original fear engram that drives freezing.

Collectively, these results indicate that the DG ensemble activated during exposure to a stressed cagemate includes a previously established functional fear engram, while the active BLA ensemble is not composed of fear-driving cells.

Conclusion

Memory recall is a malleable phenomenon that can be altered by intervening experiences, as associated context or cues can reactivate engrams and thus make them labile during incubation (35–37, 49). In this study, we discovered that even in the absence of associated reminders, salient social encounters can strengthen a preexisting fear memory in males, but not in females. We explored the role of endogenous cellular reactivation of FC ensembles in the hippocampus and amygdala during subsequent social vs. nonsocial salient events. While the two forms of socially salient events induced reactivation of the fear ensemble in the DG, the two forms of nonsocial physical stress did not cause reactivation. Unlike in the DG, reactivation in the BLA was not associated with the social, memory-enhancing experiences. To determine the functional nature of the ensembles activated during the social experiences, we optogenetically tagged these cells and artificially stimulated them with light in neutral conditions. We found that light-induced stimulation caused fear behaviors only when mice had been previously fear-conditioned and when the cells stimulated were tagged during the social experience, suggesting that the ensembles reactivated by socially salient events are fear-driving engrams. Thus, we propose that DG engram reactivation provides a mechanism for stressful social experience to potentiate negative memories. Future studies are necessary to confirm the causal role of engram reactivation with an activation-blocking strategy such as chemogenetics while avoiding potentially confounding compensatory effects (50, 51).

For both humans and mice, healthy social conditions include not only positive but also moderately stressful interactions. While extreme social stress can impair memory capabilities (8), a rich social life can protect (7) and enhance (5) memory. Although this enriching effect on learning and memory is often discussed as a function of positive social support, our findings suggest that mildly negative social exposure to conspecifics' stress also plays an important role in strengthening preexisting memory. From an evolutionary perspective, a stressed conspecific or their ambient auditory–olfactory emissions might signal a dangerous situation in which it is adaptive to hone one's own memories to guide decision making. Altogether, our findings provide evidence that the mnemonic contents of a social animal's brain are modulated throughout the course of social experiences, and we anticipate ensuing studies to unravel the circuitry bridging social sensory inputs and preexisting hippocampal engrams.

Materials and Methods

All mouse procedures were approved by the Boston University Animal Care and Use Committee.

Surgery. For all surgeries, mice were initially anesthetized under 3.5% isoflurane inhalation and then maintained during surgery at 1.0 to 2.0% isoflurane inhalation through stereotaxic nosecone delivery. Ophthalmic ointment was applied to both eyes to provide adequate lubrication and prevent corneal damage. The hair above the surgical site was removed with scissors and subsequently cleaned with alternating applications of betadine solution and 70% ethanol. Lidocaine HCl (2.0%) was injected subcutaneously as local analgesia prior to 10- to 15-mm mid-sagittal incision of the skin. For optogenetic implant surgeries, two bone anchor screws were secured into the cranium, one anterior and one posterior to the target injection and fiber placement sites. All animals then received bilateral craniotomies with a 0.6-mm drill bit for dDG and BLA injections. For all dDG and BLA surgeries, a 10-μL airtight Hamilton syringe with attached 33-gauge beveled needle was lowered to the coordinates for the DG of −2.2 mm anteroposterior (AP), ±1.3 mm mediolateral (ML), and −2.0 mm dorsoventral (DV), and for the BLA of −1.35 mm AP, ±3.25 mm ML, and −5.0 mm DV. All coordinates are given relative to bregma (mm). For overlap surgeries, a volume of 300 nL of AAV9-c-Fos-tTA (tetracycline transactivator) mixed with AAV9-TRE (tetracycline response element-EYFP) was bilaterally injected at 200 nL/min using a microinfusion pump for each coordinate (2 × 300 nL for dDG; 2 × 300 nL for BLA) (UMP3; World Precision Instruments). After the injection was complete, the needle was left in place 2 min prior to incremental retraction of the needle from the brain. For dDG or BLA optogenetic surgeries, a 300-nL viral mixture of AAV9-cFos-tTa + AAV9-TRE-ChR2-EYFP was bilaterally injected into the dDG or BLA (separate surgeries and animals for

each brain region; see overlap surgeries for coordinates and the procedure for injection). Following viral injection, bilateral optical fibers (200-μm core diameter; Doric Lenses) were placed 0.4 mm above the injection sites (dDG: −1.6 mm DV; BLA: −4.6 mm DV). The implants were secured to the skull with a layer of adhesive cement (C&M Metabond) followed by multiple layers of dental cement (Stoelting). Mice were injected with a 0.1 mg/kg intraperitoneal dose of buprenorphine (volume dependent on the weight of the animal) and placed in a recovery cage atop a heating pad until recovered from anesthesia. Viral targeting was confirmed by histological study and only animals with proper viral expression were utilized for data analysis.

Immunohistochemistry. Mice were overdosed with 3% isoflurane and perfused transcardially with cold (4 °C) phosphate-buffered saline (PBS) followed by 4% paraformaldehyde (PFA) in PBS. Brains were extracted and kept in PFA at 4 °C for 24 to 48 h and then transferred to PBS solution. Brains were sectioned into 50-μm-thick coronal sections with a vibratome and collected in cold PBS. Sections were blocked for 1 to 2 h at room temperature in PBS combined with 0.2% Triton (PBST) and 5% normal goat serum (NGS) on a shaker. Sections were incubated in primary antibody (1:1,000 rabbit anti-cFos [SySy]; 1:5,000 chicken anti-GFP [Invitrogen]) made in PBST/NGS at 4 °C for 48 h. Sections then underwent three washes in PBST for 10 min each, followed by a 2-h incubation period at room temperature with secondary antibody (1:200 Alexa 555 anti-rabbit [Invitrogen]; 1:200 Alexa 488 anti-chicken [Invitrogen]) made in PBST/NGS. Sections then underwent three more wash cycles in PBST. Sections were mounted onto microscope slides (VWR International). Vectashield HardSet Mounting Medium with DAPI (Vector Laboratories) was applied and slides were coverslipped and allowed to dry overnight. Once dry, slides were sealed with clear nail polish on each edge and stored in a slide box in the refrigerator. If not mounted immediately, sections were stored in PBS at 4 °C.

Behavior.
Fear conditioning. FC for all experiments took place in an 18.5 × 18 × 21.5–cm chamber with aluminum side walls and Plexiglas front and rear walls (context A). Each cage animal was placed in a separate chamber (4) and received shocks in parallel during the session. The session consisted of four shocks over a time span of 500 s (shocks at 198, 278, 358, and 438 s). Depending on the experiment, the length and strength of the shock varied. For the experiments without extinction training (recall 24 h after the social session), the four shocks were 1 s each at 1 mA. For the experiments with extinction, in order to obtain homogeneous and reliable fear responses at a more remote time point, more intense FC was utilized, with shocks at 1.5 mA for 2 s. After the session, animals were placed back into their home cage and in an isolated holding area until all animals in a cohort had been fear-conditioned.

Extinction training. Animals were placed into context A (see above) for a duration of 30 min on the day following FC. A second extinction training session occurred the next day (30 min). All animals in a cage of four underwent extinction training simultaneously. After the session, animals were placed back into their home cage and in an isolated holding area until all animals in a cohort had undergone extinction training.

Extinction test/extinction attenuation. Animals were placed into context A for a duration of 5 min. The extinction test was used to assess successful extinction and occurred on the day following the second session of extinction training, while the extinction attenuation assay was used to quantify freezing levels on the day following optogenetic stimulation. Similar to FC and extinction training, all animals in a cage of four underwent testing simultaneously and were placed back into their home cage and in an isolated holding area until all animals in a cohort were tested.

Recall test. For the recall test, animals were placed into context A for a duration of 5 min. As in FC and extinction training, all animals in a cage of four underwent testing simultaneously and were placed back into their home cage and in an isolated holding area until all animals in a cohort were tested.

Generalization. To assess generalization, 24 h after the recall session, animals were placed into a 18.5 × 18 × 21.5–cm chamber with vertical black and white striped (3-cm-width) sides, a plastic container holding gauze soaked in almond extract under the chamber floor, and red light as room illumination (context B) for a duration of 5 min. All animals in a cage of four underwent testing simultaneously and were placed back into their home cage and in an isolated holding area until all animals in a cohort were tested.

Immediate shock. Immediate shock was administered in context B (see above). The animal received a single 1.5-mA shock if after extinction or 1-mA shock if without extinction, beginning 1 s after trial initiation and lasting 2 s, followed by 57 s in the chamber, for a total duration of 60 s.

Juvenile intruder/cagemate control. Animals were removed from the home cage and placed into a separate, clean cage with access to food and water. The lid of the cage and the feeder were removed from the home cage, which served as the interaction chamber. An experimental mouse was placed back into the home cage and allowed 1 min to acclimate. An unfamiliar younger (postnatal days 43 to 49) intruder mouse was placed into the home cage for 10 min of interaction with the experimental resident mouse; younger mice were used to avoid confounding effects of mutual aggression (25, 26). A clear acrylic top was placed over the home cage during interaction. This was repeated for each experimental cage animal. A different intruder mouse was used in each session. After each session, both mice were removed from the home cage and placed into a separate holding cage for their respective group. For cagemate control experiments, a cagemate of the resident mouse was used for interaction in lieu of the unfamiliar intruder. The social session was conducted with a procedure otherwise identical to that used for juvenile intruder.

Full interaction. The lid of the cage and the feeder were removed for social interaction and a clear acrylic top was placed over the home cage. The recently shocked cagemate was then placed into the cage and all animals were left in the testing room for 1 h of social interaction. After 1 h, the home cage was returned to its normal condition.

One-way mirror/mirror no mouse control/opaque control. Mirror inserts were created out of laminated cardboard and one-way mirror material (OuBay). Wooden dowels were placed on the bottom to support the structure. Dimensions were based to fit tightly into the cage (7 × 11 × 5 in) to separate the container into two sections (a smaller area for the recently shocked cagemate and a larger area for the rest of the cagemates). The lid of the cage and the feeder were removed for social interaction and a clear acrylic top was placed over the home cage. In order to enhance the effect of the mirror by creating a large light difference, black covers were created to cover the section of the cage with the recently shocked cagemate. Refer to *SI Appendix,* Fig. S1 for a visual representation of the setup. After immediate shock, the recently shocked cagemate was immediately placed into the section opposite of and separate from the other cagemates. Animals were left in the testing room for 1 h of social interaction. After 1 h, the recently shocked cagemate was removed and immediately euthanized by overdose with sodium pentobarbital to ensure any subsequent effects were due to the manipulation rather than any social interaction afterward, and the home cage was returned to its normal condition. For the mirror no mouse control, all procedural steps were identical to the one-way mirror experiments, except that there was no shocked cagemate placed on the other side of the mirror. For opaque control experiments, the one-way mirror insert was altered through the addition of a black insert on the side of the shocked cagemate so that the wall was bidirectionally blocking visual input from the other side. Social interaction was conducted with a procedure otherwise identical to that used for one-way mirror experiments.

Social buffering. To determine the impact of social buffering of the shocked cagemate, subjects experienced the same protocol as one-way mirror except that one of the cagemates was placed behind the mirror insert during the immediate shock, so that the shocked mouse was able to directly interact with this cagemate during the following 1 h. Afterward, both the shocked cagemate and "bufferer" mouse were placed into a new cage before the insert was removed to ensure the effect on experimental mice was limited to the time window of the manipulation.

Restraint/tube control. One at a time, animals were removed from the home cage and enclosed in a plastic restraint tube containing holes to permit airflow. The tube was then placed in the center of a clean cage for a duration of 2 min. At the end of the 2 min, the animal was released from the tube into one separate clean cage where all the mice were reunited post restraint. For the tube control test, all animals remained in the home cage and a clean restraint tube was placed into the home cage for a duration of 2 min.

Female exposure. One at a time, animals were removed from the home cage and placed into a separate, clean cage for 10 min of interaction with an unfamiliar female conspecific. To lessen the females' stress-induced resistance to mating, some of the females' bedding was sprinkled into the cage and the females were

habituated to the new environment for 1 min prior to introduction of the experimental male. A clear acrylic top was placed over the cage during interaction. This was repeated for each experimental cage animal. A different female was used in each session. After each session, both mice were removed from the interaction cage and placed in a new cage, so that naïve animals could not interact with those that had already gone through the experience.

Optogenetic Stimulation. The optogenetic stimulation session occurred 24 h after the tagging experience (one-way mirror). Prior to the start of the session, optogenetic patch cords were tested to ensure a minimum 10-mA laser output. Mice were given stimulation in a separate room from context A or B. For stimulation, the mice were attached to the optogenetic cords in the palm of A.B.F.'s hand and placed into a striped acrylic chamber with either white or dimmed white + red light and either almond or orange scent (context C). The session lasted 8 min and consisted of four alternating 2-min periods of laser stimulation [off/on/off/on; dDG: 450 nm, 20 Hz, 10-ms pulse width (52); BLA: 450 nm, 4 and 20 Hz, 10-ms pulse width (53)]. The BLA group received 4- and 20-Hz stimulation counterbalanced in different contexts (orange vs. almond scent, white vs. red light) separated by about 1.5 h.

Behavior Scoring.
FreezeFrame. Videos of behavioral sessions were obtained using cameras secured to the chamber either above or to the side of the subject. For extinction, extinction test, and recall sessions, FreezeFrame/View (Coulbourn Instruments) was used to score freezing behavior, defined as 1.25 s of animal immobility.
Manual scoring. For optogenetic sessions, due to cord movement and lighting conditions interfering with automated scoring, all freezing and grooming quantification was done manually. This was then converted to a percentage of time that the mouse spent freezing within the bins of stimulation in the session. Each video was scored for grooming by H.L., and for freezing by two separate observers (A.B.F. and H.L. or A.B.F. and R.H.C.) whose scores were averaged to mitigate variation in bout length perception. Grooming was defined as any syntactic-chain cephalocaudal grooming, scratching, licking, or other observable forms of nonchain self-grooming performed by the animal (40). Freezing was defined as any observable complete cessation of movement, other than breathing, by the animal.

Imaging and Cell Counting. All coronal brain slices were imaged through a Zeiss LSM 800 epifluorescence microscope with a 20×/0.8 numerical aperture objective using Zen2.3 software. Images of the BLA were captured in a 2 × 2 tile (640 × 640–μm) Z stack. Images of the DG were captured in a 4 × 2 tile (1,280 × 640–μm) Z stack. DAPI and green fluorescent protein (GFP) were imaged as separate channels for target verification and ensemble size quantification. For overlap counts, DAPI, cFos, and GFP were imaged (DAPI and cFos simultaneously and GFP as a separate channel). Three or four different slices were imaged for each animal for averaging.
Fiji software. Images were processed for greater clarity before quantification. The Subtract Background tool was used to enhance the contrast of cells to the background, and Despeckle was used to minimize noise that may interfere with quantification. Regions of interest were selected using Freehand Selection so that only cells within the brain region would be analyzed. The DAPI channel was segmented using a custom pipeline involving 3D Object Counter. The cFos and GFP channels were initially segmented using a custom pipeline utilizing the 3D Iterative Thresholding tool of 3D ImageSuite (54). Once cells segmented, the Z stacks were Z-projected into a single slice image and saved.
CellProfiler. Segmented images of DAPI, cFos, and GFP were loaded into CellProfiler and run through a pipeline that identified cells with more stringent

parameters of size and shape. For overlap quantification, the final step in the pipeline counted all identified objects between the cFos and GFP images that had an overlap of greater than 80%.
Cell quantification and analysis. Once cells were counted, the relative amounts of cFos$^+$ only, GFP$^+$ only, and cFos$^+$GFP$^+$ (overlap) cells in each slice were normalized over the total amount of DAPI cells present (cFos$^+$/DAPI, GFP$^+$/DAPI, overlap/DAPI). Chance of an overlap was defined as (cFos$^+$/DAPI) × (GFP$^+$/DAPI). Overlap over chance was then calculated by dividing overlap/DAPI by the chance overlap calculated in the previous step.

Data Analysis.
Freezing during recall and generalization. Behavioral and histological data were analyzed using Prism version 9.1.1 for Mac OS (GraphPad Software). For the recall behavior, we aimed to compare freezing levels between a neutral control group and each manipulated group. As SDs passed Brown–Forsythe's and Bartlett's tests for nonsignificantly different SDs and all normality tests, we conducted ordinary one-way ANOVAs followed by post hoc comparisons with the neutral group using Holm–Sidak's correction for multiple comparisons. For generalization behavior, we compared the generalization scores ([recall freezing − context B freezing]/recall freezing) of each group with those of the neutral group. When distributions did not pass the Anderson–Darling test for normality, we conducted the Kruskal–Wallis test followed by Dunn's multiple comparisons with the neutral group.
Freezing and self-grooming during optogenetic stimulation. For the DG optogenetic data, we aimed to determine the effects and interactions of optogenetic stimulation, prior FC, and social experience during the tagging window. We therefore used two-way repeated-measures ANOVAs followed by pairwise multiple comparisons between stimulation trials within each of the three groups with Holm–Sidak's correction. These same tests were used for the BLA optogenetic data, where we aimed to determine the effects and interactions of optogenetic stimulation, frequency of stimulation, and prior FC.
Cellular overlaps. To quantify the degree of overlap in cellular populations active during FC and each of our conditions the following day, we aimed to compare the number of overlaps in each brain region with that expected by chance based on the size of the two populations. We therefore normalized overlaps over chance as described above in *Cell Quantification and Analysis* and compared with chance with one-sample t tests. In order to compare the levels of activity during each of the salient and control conditions, we also performed one-way ANOVAs on % cFos/DAPI in each brain region, followed by Holm–Sidak's multiple comparisons.

Data Availability. All study data are included in the article and/or supporting information.

Author affiliations: [a]Department of Psychological and Brain Sciences, Boston University, Boston, MA, 02215; [b]Department of Molecular and Cellular Biology, Harvard University, Cambridge, MA, 02138; [c]Boston University School of Medicine, Boston, MA, 02118; [d]Chemical Biology and Therapeutic Sciences, The Broad Institute of MIT and Harvard, Cambridge, MA, 02142; and [e]Nash Department of Neuroscience, Icahn School of Medicine at Mount Sinai, New York, NY, 10029

1. J. A. Williamson, "Social support, mood, and relationship satisfaction at the trait and social levels," PhD thesis, University of Iowa (2015).
2. R. D. Reavis, L. J. Donohue, M. C. Upchurch, Friendship, negative peer experiences, and daily positive and negative mood. *Soc. Dev.* **24**, 833–851 (2015).
3. R. Neumann, F. Strack, "Mood contagion": The automatic transfer of mood between persons. *J. Pers. Soc. Psychol.* **79**, 211–223 (2000).
4. E. T. Higgins, J. A. Bargh, Social cognition and social perception. *Annu. Rev. Psychol.* **38**, 369–425 (1987).
5. V. R. Heimer-McGinn, T. B. Wise, B. M. Hemmer, J. N. T. Dayaw, V. L. Templer, Social housing enhances acquisition of task set independently of environmental enrichment: A longitudinal study in the Barnes maze. *Learn. Behav.* **48**, 322–334 (2020).
6. V. Doulames, S. Lee, T. B. Shea, Environmental enrichment and social interaction improve cognitive function and decrease reactive oxidative species in normal adult mice. *Int. J. Neurosci.* **124**, 369–376 (2014).
7. T. J. Dause, E. D. Kirby, Aging gracefully: Social engagement joins exercise and enrichment as a key lifestyle factor in resistance to age-related cognitive decline. *Neural Regen. Res.* **14**, 39–42 (2019).
8. S. Kuhlmann, M. Piel, O. T. Wolf, Impaired memory retrieval after psychosocial stress in healthy young men. *J. Neurosci.* **25**, 2977–2982 (2005).
9. T. Peleh, A. Eltokhi, C. Pitzer, Longitudinal analysis of ultrasonic vocalizations in mice from infancy to adolescence: Insights into the vocal repertoire of three wild-type strains in two different social contexts. *PLoS One* **14**, e0220238 (2019).
10. G. A. Castellucci, D. Calbick, D. McCormick, The temporal organization of mouse ultrasonic vocalizations. *PLoS One* **13**, e0199929 (2018).
11. M. Wöhr, D. Seffer, R. K. W. Schwarting, Studying socio-affective communication in rats through playback of ultrasonic vocalizations. *Curr. Protoc. Neurosci.* **75**, 8–35 (2016).
12. N. Simola, S. M. Brudzynski, "Repertoire and biological function of ultrasonic vocalizations in adolescent and adult rats" in *Handbook of Ultrasonic Vocalization–A Window into the Emotional Brain*, S. M. Brudzynski, Ed. (Elsevier, 2018), pp. 177–186.

13. E. Biasi, L. Silvotti, R. Tirindelli, Pheromone detection in rodents. *Neuroreport* **12**, A81–A84 (2001).
14. T. W. Bredy, M. Barad, Social modulation of associative fear learning by pheromone communication. *Learn. Mem.* **16**, 12–18 (2008).
15. C. L. Ebbesen, E. Bobrov, R. P. Rao, M. Brecht, Highly structured, partner-sex- and subject-sex-dependent cortical responses during social facial touch. *Nat. Commun.* **10**, 4634 (2019).
16. M. J. Hertenstein, J. M. Verkamp, A. M. Kerestes, R. M. Holmes, The communicative functions of touch in humans, nonhuman primates, and rats: A review and synthesis of the empirical research. *Genet. Soc. Gen. Psychol. Monogr.* **132**, 5–94 (2006).
17. N. Liu *et al.*, Single housing-induced effects on cognitive impairment and depression-like behavior in male and female mice involve neuroplasticity-related signaling. *Eur. J. Neurosci.* **52**, 2694–2704 (2020).
18. A. Montagrin, C. Saiote, D. Schiller, The social hippocampus. *Hippocampus* **28**, 672–679 (2018).
19. K. M. Gothard, Multidimensional processing in the amygdala. *Nat. Rev. Neurosci.* **21**, 565–575 (2020).
20. P. Davis, L. G. Reijmers, The dynamic nature of fear engrams in the basolateral amygdala. *Brain Res. Bull.* **141**, 44–49 (2018).
21. P. H. Janak, K. M. Tye, From circuits to behaviour in the amygdala. *Nature* **517**, 284–292 (2015).
22. S. Duvarci, D. Pare, Amygdala microcircuits controlling learned fear. *Neuron* **82**, 966–980 (2014).
23. X. Sun *et al.*, Functionally distinct neuronal ensembles within the memory engram. *Cell* **181**, 410–423.e17 (2020).
24. S. A. Josselyn, S. Tonegawa, Memory engrams: Recalling the past and imagining the future. *Science* **367**, eaaw4325 (2020).
25. A. C. Felix-Ortiz, K. M. Tye, Amygdala inputs to the ventral hippocampus bidirectionally modulate social behavior. *J. Neurosci.* **34**, 586–595 (2014).
26. E. B. Defensor, M. J. Corley, R. J. Blanchard, D. C. Blanchard, Facial expressions of mice in aggressive and fearful contexts. *Physiol. Behav.* **107**, 680–685 (2012).
27. J. W. Clark, S. P. A. Drummond, D. Hoyer, L. H. Jacobson, Sex differences in mouse models of fear inhibition: Fear extinction, safety learning, and fear-safety discrimination. *Br. J. Pharmacol.* **176**, 4149–4158 (2019).
28. A. Uwaya *et al.*, Acute immobilization stress following contextual fear conditioning reduces fear memory: Timing is essential. *Behav. Brain Funct.* **12**, 8 (2016).
29. Y. E. Wu *et al.*, Neural control of affiliative touch in prosocial interaction. *Nature* **599**, 262–267 (2021).
30. M. B. Hennessy, S. Kaiser, N. Sachser, Social buffering of the stress response: Diversity, mechanisms, and functions. *Front. Neuroendocrinol.* **30**, 470–482 (2009).
31. Z. Donaldson *et al.*, 25.2 Social buffering of conditioned and innate fear responses. *J. Am. Acad. Child Adolesc. Psychiatry* **10**, S297 (2016).
32. F. Stefanini *et al.*, A distributed neural code in the dentate gyrus and in CA1. *Neuron* **107**, 703–716.e4 (2020).
33. K. Z. Tanaka *et al.*, Cortical representations are reinstated by the hippocampus during memory retrieval. *Neuron* **84**, 347–354 (2014).
34. B. K. Chen *et al.*, Artificially enhancing and suppressing hippocampus-mediated memories. *Curr. Biol.* **29**, 1885–1894.e4 (2019).
35. S. J. Sara, Strengthening the shaky trace through retrieval. *Nat. Rev. Neurosci.* **1**, 212–213 (2000).
36. M. C. Inda, E. V. Muravieva, C. M. Alberini, Memory retrieval and the passage of time: From reconsolidation and strengthening to extinction. *J. Neurosci.* **31**, 1635–1643 (2011).
37. J. Kim, J.-T. Kwon, H.-S. Kim, S. A. Josselyn, J.-H. Han, Memory recall and modifications by activating neurons with elevated CREB. *Nat. Neurosci.* **17**, 65–72 (2014).
38. S. Ramirez *et al.*, Creating a false memory in the hippocampus. *Science* **341**, 387–391 (2013).
39. R. L. Redondo *et al.*, Bidirectional switch of the valence associated with a hippocampal contextual memory engram. *Nature* **513**, 426–430 (2014).
40. A. V. Kalueff *et al.*, Neurobiology of rodent self-grooming and its value for translational neuroscience. *Nat. Rev. Neurosci.* **17**, 45–59 (2016).
41. A. Siegmund, C. T. Wotjak, A mouse model of posttraumatic stress disorder that distinguishes between conditioned and sensitised fear. *J. Psychiatr. Res.* **41**, 848–860 (2007).
42. A. D. LaMotte, C. T. Taft, R. P. Weatherill, C. I. Eckhardt, Social skills deficits as a mediator between PTSD symptoms and intimate partner aggression in returning veterans. *J. Fam. Psychol.* **31**, 105–110 (2017).
43. J. M. Cisler *et al.*, Brain and behavioral evidence for altered social learning mechanisms among women with assault-related posttraumatic stress disorder. *J. Psychiatr. Res.* **63**, 75–83 (2015).
44. C. E. Dutton, S. M. Rojas, C. L. Badour, S. G. Wanklyn, M. T. Feldner, Posttraumatic stress disorder and suicidal behavior: Indirect effects of impaired social functioning. *Arch. Suicide Res.* **20**, 567–579 (2016).
45. D. J. Cai *et al.*, A shared neural ensemble links distinct contextual memories encoded close in time. *Nature* **534**, 115–118 (2016).
46. B. D. Yetton, D. J. Cai, V. I. Spoormaker, A. J. Silva, S. C. Mednick, Human memories can be linked by temporal proximity. *Front. Hum. Neurosci.* **13**, 315 (2019).
47. S.-C. Lee, A. Amir, D. Haufler, D. Pare, Differential recruitment of competing valence-related amygdala networks during anxiety. *Neuron* **96**, 81–88.e5 (2017).
48. P. A. Rodríguez Manzanares, N. A. Isoardi, H. F. Carrer, V. A. Molina, Previous stress facilitates fear memory, attenuates GABAergic inhibition, and increases synaptic plasticity in the rat basolateral amygdala. *J. Neurosci.* **25**, 8725–8734 (2005).
49. C. L. Pickens, S. A. Golden, T. Adams-Deutsch, S. G. Nair, Y. Shaham, Long-lasting incubation of conditioned fear in rats. *Biol. Psychiatry* **65**, 881–886 (2009).
50. E. J. Campbell, N. J. Marchant, The use of chemogenetics in behavioural neuroscience: Receptor variants, targeting approaches and caveats. *Br. J. Pharmacol.* **175**, 994–1003 (2018).
51. S. L. Grella, A. H. Fortin, O. McKissick, H. Leblanc, S. Ramirez, Odor modulates the temporal dynamics of fear memory consolidation. *Learn. Mem.* **27**, 150–163 (2020).
52. X. Liu *et al.*, Optogenetic stimulation of a hippocampal engram activates fear memory recall. *Nature* **484**, 381–385 (2012).
53. D. S. Roy *et al.*, Brain-wide mapping of contextual fear memory engram ensembles supports the dispersed engram complex hypothesis. bioRxiv [Preprint] (2019). https://doi.org/10.1101/668483 (Accessed 12 October 2020).
54. J. Ollion, J. Cochennec, F. Loll, C. Escudé, T. Boudier, TANGO: A generic tool for high-throughput 3D image analysis for studying nuclear organization. *Bioinformatics* **29**, 1840–1841 (2013).